

LETTERS

Pressure Stabilization and Solvation Thermodynamics of a Hemiketal Reaction Intermediate

Alan D. Gift and Dor Ben-Amotz*

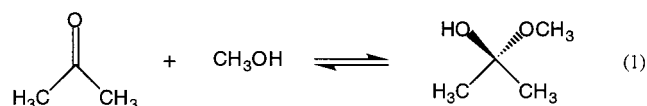
Department of Chemistry, Purdue University, West Lafayette, Indiana 47907

Received: August 4, 2000; In Final Form: October 19, 2000

This work reports the first pressure stabilization of a hemiketal intermediate, 2-methoxy-2-propanol, formed in the reaction of acetone and methanol, observed using Raman spectroscopy. Acetone dissolved in methanol is found to undergo a two-step reaction, with the ketal 2,2-dimethoxy-propane as the final product and the hemiketal observed as an intermediate. In a more dilute stoichiometric mixture of acetone and methanol in liquid tetrahydrofuran (THF), quantitative formation of the hemiketal is observed at pressures above 2 GPa. The complete set of reaction thermodynamic functions (ΔH° , ΔV° , ΔS° , ΔG° , ΔU° , ΔA°) is obtained for the hemiketal formation reaction in THF as a function of temperature and pressure and compared with previous measurements of ΔH° , ΔS° , and ΔG° for acetone dissolved in methanol. Comparisons with quantum calculations for the isolated reactant and product species are used to completely quantitate the effects of solvation on the hemiketal formation reaction.

Introduction

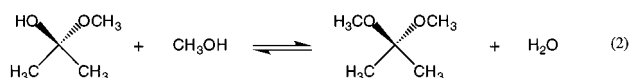
The reaction of carbonyl and hydroxyl groups plays a central role in a wide variety of important organic and biological processes.¹⁻⁵ A prime example is the intramolecular hemiacetal formation responsible for the cyclization of glucose. More generally, acetals and ketals are formed from the reaction of aldehydes or ketones, respectively, with alcohols. The hemiacetal or hemiketal species, which are thought to be intermediates in these reactions, are typically unstable under ambient conditions and thus have rarely been studied directly.² We report the first quantitative conversion of acetone and methanol to the hemiketal 2-methoxy-2-propanol (MP, eq 1) dissolved in tetrahydrofuran (THF) under high pressure.



Calibrated Raman peak area measurements are used to determine the pressure and temperature dependence of the hemiketal formation equilibrium constant. The results are used to completely characterize the thermodynamics of this reaction by determining Gibbs free energy (ΔG°), enthalpy (ΔH°), entropy (ΔS°), partial molar volume (ΔV°), internal energy (ΔU°), and helmholtz free energy (ΔA°) vs P and T . Comparison with quantum calculations for the isolated reactant and product species yields the solvent excess contribution to the reaction thermodynamics as a function of temperature and pressure. To the best of our knowledge, this is the first example of such a complete thermodynamic analysis of the effects of solvation on any chemical reaction.

In a neutral solution, the hemiketal formation equilibrium strongly favors the reactants (1 M solution of acetone in methanol contains 7.32 mM of MP).² When this reaction takes place in the presence of an acid catalyst, along with the removal of water, the reaction equilibrium is shifted to the formation of

the thermodynamically stable ketal product 2,2-dimethoxypropane (DMP, available commercially as a 98% pure liquid, eq 2).



Previous studies of reaction 2 have used NMR spectroscopy^{2,6} and UV spectroscopy^{7,8} to obtain the thermodynamics of the ketal formation reaction. The trace presence of hemiketal due to reaction 1 has been detected by NMR in an ambient mixture of acetone and methanol. This was used to determine the equilibrium constant for the hemiketal formation as a function of temperature and derive the reaction thermodynamic functions $\Delta H^\circ = -14.1$ kJ/mol, $\Delta S^\circ = -88.6$ J/(Kmol), and $\Delta G^\circ = 12.3$ kJ/mol in this ambient solution.² In addition, ab initio calculations by Wiberg et al. predict $\Delta U^\circ(\text{gas}) = -32.4$ kJ/mol in the vapor phase, which implies $\Delta H^\circ(\text{gas}) \sim -35$ kJ/mol.² Although these previous studies are not sufficient to quantify the complete thermodynamics of the reaction, comparison of the gas and solution ΔH° values clearly indicates the significant effect of solvation on this reaction.

Experimental Section

The present temperature and pressure studies were performed using Raman spectroscopy to monitor the concentrations of acetone and the hemiketal. Dispersive micro-Raman measurements were carried out using a He–Ne excitation laser (20 mW, 632.8 nm), as described elsewhere.⁹ Pressure and temperature were varied by placing the sample in a diamond anvil cell (DAC) immersed in a variable temperature oil bath. The solution pressure was determined using ruby fluorescence,¹⁰ and temperature was measured using a thermocouple placed in the oil bath next to the DAC.

Reagent grade acetone, methanol, THF, and DMP were used as received from Aldrich. Raman spectra of each of these compounds, in their pure liquid state, were measured and used to assist in the assignment of vibrational bands appearing in the reactive mixture.

Results and Discussion

Preliminary high-pressure measurements were performed on a solution of acetone in excess methanol (with a solute mole fraction of about 0.2). At ambient conditions, the only observable peak in the 725 to 825 cm^{-1} range was the C–C stretch of acetone at 788 cm^{-1} . When the pressure was increased, a new peak was formed rapidly at about 759 cm^{-1} , while the acetone peak at 788 cm^{-1} decreased in intensity. The transformation of the spectrum occurred within a few seconds after the pressure was increased, and equilibrated in less than one minute. When the sample was allowed to sit at high pressure for 1 day, the peak at 759 cm^{-1} decreased in intensity and a new peak formed at 739 cm^{-1} , indicating the slow transformation to a second product. When the pressure was decreased back to 1 atm, the 759 cm^{-1} product reverted to acetone (759 cm^{-1}), while the 739 cm^{-1} product remained. The Raman spectrum of pure DMP [Aldrich D13,680–8] has a strong C–C stretching vibration at 730 cm^{-1} in the 1 atm liquid state, which corresponds well with the 739 cm^{-1} peak after a pressure-induced frequency shift is taken into consideration.¹¹ Furthermore, quantum calculations using B3LYP/6-31G* theory level predict strong Raman active C–C stretch vibrations at 786, 757, and 737 cm^{-1} for acetone, MP and DMP, respectively. These

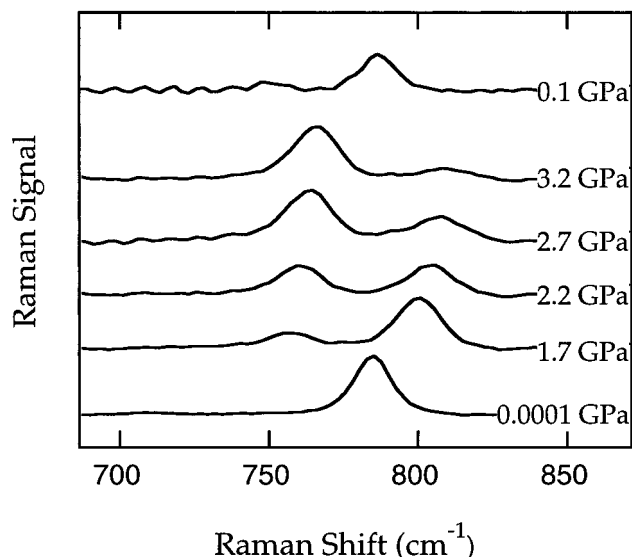


Figure 1. Raman spectra of a solution of acetone and methanol dissolved in tetrahydrofuran reveal reversible spectral changes attributed to pressure induced hemiketal formation. Spectra were collected over a series of increasing pressures followed by a pressure decrease (spectra are shifted vertically for clarity). The C–C stretch of acetone at ~ 780 cm^{-1} shifts to 800 cm^{-1} with increasing pressure, as the hemiketal C–C peak grows in at ~ 760 cm^{-1} .

results strongly suggest the assignment of the rapidly formed species to MP and the more slowly formed product to DMP.

Further confirmation of the above assignments was obtained by pressure cycling a solution of acetone and methanol dissolved in THF (with mole fractions of about 0.12 for each solute). In this case, near quantitative conversion of acetone to a product with a Raman band around 760 cm^{-1} was achieved at pressures over 2 GPa, as illustrated by the Raman spectra shown in Figure 1. These spectra were collected sequentially (from bottom to top) during the pressurization and then depressurization of the sample. Note that in addition to the appearance and disappearance of peaks, there is an observable pressure shift in the vibrational frequencies of each species, which is consistent with the pressure-induced frequency shift of about 7 $\text{cm}^{-1}/\text{GPa}$ for the C–C stretch of acetone.¹¹ The recovery of the acetone spectrum upon depressurization thus supports our assignment of the high-pressure product is the hemiketal (MP), since the ketal (DMP) is stable at 1 atm.

Thus, in a solution of acetone and methanol in THF, quantitative conversion to the hemiketal is observed without appreciable production of the ketal. Acetone dissolved in methanol, on the other hand, undergoes sequential formation of the hemiketal followed by the ketal (undoubtedly driven by the presence of excess methanol). These results not only demonstrate the possibility of quantitatively converting acetone and methanol to an equilibrated hemiketal, but also confirm that the hemiketal is indeed an intermediate in the reaction pathway leading to the ketal.

To quantitate the reaction thermodynamics of the hemiketal reaction, further measurements were performed on a similar THF solution of acetone and methanol at four temperatures and three pressures. Peak areas were determined for the C–C stretching bands of acetone and MP in the 725–825 cm^{-1} region (Figure 1) and for the solvent THF. The acetone and MP peak areas were divided by the THF peak area to provide an internal standard. This normalization procedure has the effect of compensating for changes in laser power, collection efficiency, and changing sample thickness with increasing pressure. The

TABLE 1: Reaction Thermodynamics for the Formation of Hemiketal from Acetone and Methanol

reaction thermodynamics (at 25 °C and 1 M concentration)	in THF at 1 atm	in THF at 2 GPa	in methanol at 1 atm	gas phase at 1 M	solvent excess thermodynamic functions	
					in THF at 1 atm	in THF at 2 GPa
ΔG° (kJ/mol)	15.1	4.0	12.3	13.7 ^b	1.4	-9.7
ΔH° (kJ/mol)	-12.9	-25.2	-14.1	-34.9 ^b	22.0	9.7
ΔS° (J/Kmol)	-94	-98	-89	-163	69	65
ΔV° (cm ³ /mol)	6.0	6.0	—	0	6	6
ΔU° (kJ/mol)	-12.9	-12.9	—	-32.4 ^d	19.5	19.5
ΔA° (kJ/mol)	15.1	16.3	—	16.2 ^b	-1.1	0.1

^a Derived from NMR measurements of Wiberg et al.² ^b Values obtained using ΔU° , $T\Delta S^\circ$, the ideal gas law ($PV = nRT$), and standard thermodynamic relations.¹⁴ ^c Quantum calculation using CBS-4 extrapolation method (this work). ^d Quantum calculation by Wiberg et al. using CBS-4 extrapolation method.² ^e Under ideal gas 1M standard state conditions $\Delta V^\circ = (\partial\Delta G^\circ/\partial P)_T = 0$.

resulting normalized acetone peak areas were plotted as a function of the normalized MP peak areas. The slope and intercept of the resulting line, along with the known initial concentration of acetone (in molality units), were used to relate the measured peak areas to concentrations of acetone of MP at every experimental temperature and pressure. The methanol concentration was determined by subtracting the concentration of MP from the initial concentration of methanol. The resulting concentrations were converted to molarity units using the compressibility of THF, as predicted by the van der Waals–Carnahan–Starling equation of state.^{12,13} Thus the equilibrium constant, $K = [\text{MP}]/[\text{acetone}][\text{methanol}]$, was determined at each temperature and pressure.

Measurements of K as a function of both temperature and pressure were used to determine the complete set of thermodynamic functions, ΔH° , ΔG° , ΔS° , ΔV° , ΔU° , ΔA° , at a standard state concentration of 1 M. In particular, the standard state Gibbs free energy was related to K using the following expression:⁹

$$\Delta G^\circ = -RT \ln K \quad (3)$$

The remaining thermodynamic functions were derived from the corresponding standard identities.^{9,14}

$$\Delta H^\circ = -R \left(\frac{\partial \ln K}{\partial (1/T)} \right)_P \quad \Delta V^\circ = -RT \left(\frac{\partial \ln K}{\partial P} \right)_T \quad (4)$$

$$\begin{aligned} T\Delta S^\circ &= \Delta H^\circ - \Delta G^\circ \\ \Delta U^\circ &= \Delta H^\circ - P\Delta V^\circ \\ \Delta A^\circ &= \Delta U^\circ - T\Delta S^\circ \end{aligned} \quad (5)$$

In practice, the natural logarithm of the equilibrium constant at four temperatures (20, 50, 75, 100 °C) was first plotted as a function of pressure. Data points were interpolated to three fixed pressures (2.0, 2.4, and 2.8 GPa) and then graphed as a function of temperature. Figure 2 shows plots of these interpolated data points both as a function of pressure and inverse temperature. The slopes of these best fit lines shown in Figure 2 were used to experimentally determine ΔH° at each pressure and ΔV° at each temperature. The results reveal that ΔG° increases linearly with temperature and decreases linearly with pressure. The enthalpy, ΔH° , decreases with pressure but is independent of temperature, while ΔU° , ΔS° , and ΔV° are all constant within experimental error over the entire experimental temperature and pressure range.

Table 1 contains our experimental results extrapolated to 1 atm and 2 GPa, along with other experimental and theoretical values,² all pertaining to the hemiketal reaction at 25 °C (eq 1). The excess solvation thermodynamic parameters in the last column of Table 1 are obtained by subtracting the theoretical

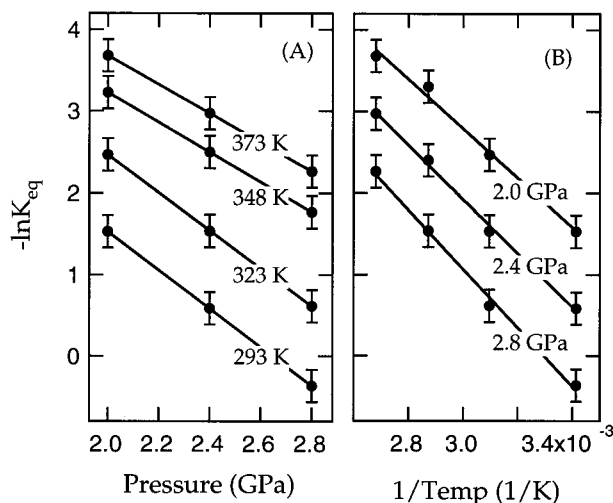


Figure 2. The logarithm of the equilibrium constant is plotted as a function of pressure (P) and inverse temperature ($1/T$). The slopes of the best fit lines yield (A) reaction volumes of $\Delta V = -5.5$, -5.3 , -6.2 , and -5.8 cm³/mole at $T = 373$, 348 , 323 , and 293 K respectively, and (B) reaction enthalpies of $\Delta H = -25.2$, -27.5 , and -30.1 kJ/mol at $P = 2.0$, 2.4 , and 2.8 GPa, respectively.

gas-phase results from our solution measurements in THF, extrapolated to 1 atm.

Some care must be exercised in interpreting the results in Table 1, in view of potential uncertainty in the experimental and/or theoretical values. The accuracies of the experimental values are believed to be about ± 2 kJ/mol, whereas those of the theoretical gas-phase results are more difficult to estimate. In particular, although the CBS-4 extrapolation method used by Wiberg² et al. is considered to yield reliable energies, we have found that much smaller negative (or even positive) gas phase ΔU° predictions may be obtained when using different ab initio algorithms and basis sets (the largest value we found was $\Delta U^\circ = +13.8$ kJ/mol, obtained using a B3LYP/6-311G** energy calculation at the B3LYP/6-31G* optimized geometry). The calculated entropy factors, $T\Delta S^\circ$, in the gas phase are found to be less sensitive to the calculation level and did not vary by more than about ± 2.0 kJ/mol (the reported value is that obtained using the same CBS-4 extrapolation method used by Wiberg² et al. to obtain the gas phase ΔU° given in Table 1).

The similarity of the thermodynamic parameters measured in the two solvents at 1 atm (THF and methanol) is noteworthy, as these are far more similar to each other than they are to the corresponding gas phase or high-pressure values. Notice that the solution results are obtained by very different experimental techniques (NMR and Raman), and the THF solution values are derived from an extrapolation of our high-pressure results

to 1 atm, whereas the equilibrium constant is far too small to allow direct Raman measurements of the hemiketal concentration.

A further important feature of the results is the similarity of the 1 atm ΔH° and ΔU° values, which also requires that ΔG° and ΔA° must be the nearly equal.¹⁴ However, when the pressure is increased to 2 GPa, the values of ΔH° and ΔU° (or ΔG° and ΔA°) diverge as a result of the increasing magnitude of $P\Delta V^\circ$. This behavior beautifully illustrates the importance of ΔV° in dictating the pressure dependence of reaction thermodynamic values. Although ΔV° typically plays a negligible role for reactions carried out under ambient conditions, it may become a dominant contribution to some high-pressure industrial processes, or even for exotic biological processes occurring in deep ocean hydrothermal vents or extraterrestrial environments.^{15,16}

The difference between the liquid and gas-phase reaction thermodynamic functions represents the solvent contribution to the chemical equilibrium (see the last few columns of Table 1). The excess potential energy of reaction, ΔU^x , indicates that the solvation energy of the reactants (acetone + methanol) and product (hemiketal) differ by about 20 kJ/mol in THF at both 1 atm. and 2 GPa. The large excess entropy of reaction, ΔS^x , implies that solvent structural rearrangement plays a significant role in solvation thermodynamics (an effect which is difficult to reproduce using dielectric continuum solvation models).^{17,18} Like ΔU^x and ΔS^x , the excess reaction volume, ΔV^x , is also approximately pressure independent. The constancy of these functions implies that there is little change in solvent structure with pressure. On the other hand, because our experiments span more than a 10 000-fold increase in pressure, the associated change in $P\Delta V^x$ produces dramatic changes in ΔH^x and ΔG^x . A further interesting feature of the excess thermodynamic results is the very small, and nearly pressure independent, value of the excess Helmholtz free energy, ΔA^x . This implies a nearly perfect cancellation of the large ΔU^x and $T\Delta S^x$, reminiscent of the well-known enthalpy–entropy compensation phenomena.^{19–21} Our results suggest that although both $\Delta H^x - T\Delta S^x$ and $\Delta U^x - T\Delta S^x$ are nearly zero at 1 atm, only the latter cancellation continues into the high-pressure regime, which may warrant a theoretical reexamination of such compensation phenomena. More generally, the sort of global excess reaction thermody-

amic results which we have presented, serve as an experimental bench-mark against which to test both fundamental solvation theories and semiempirical solvation modeling strategies.^{9,22–24}

Acknowledgment. This work was supported by the National Science Foundation (CHE-9530595).

References and Notes

- (1) March, J. *Advanced Organic Chemistry*; Wiley: New York, 1992; 889–890.
- (2) Wiberg, K. B.; Morgan, K. M.; Maltz, H. *J. Am. Chem. Soc.* **1994**, *116*, 11067–11077.
- (3) Carey, F. A.; Sunberg, R. J. *Advanced Organic Chemistry Part A: Structure and Mechanisms*, 3rd ed.; Plenum Press: New York, 1990; p 439–444.
- (4) Guthrie, J. P. *Can. J. Chem.* **1975**, *53*, 898–906.
- (5) Streitwieser, A., Jr.; Heathcock, C. H. *Introduction to Organic Chemistry*; Macmillan Publishing Co. Inc.: New York, 1976; p 368–378.
- (6) Hine, J.; Redding, R. W. *J. Org. Chem.* **1970**, *35*, 2769–2772.
- (7) Garrett, R.; Kubler, D. G. *J. Org. Chem.* **1966**, *31*, 2665–2667.
- (8) Bell, J. M.; Kubler, Sartwell, P.; Zepp, R. G. *J. Org. Chem.* **1965**, *30*, 4284–4292.
- (9) Hu, M.-H. A.; de Souza, L. E. S.; Lee, M.-R.; Ben-Amotz, D. *J. Chem. Phys.* **1999**, *110*, 2498–2507.
- (10) Piermarini, G. J.; Block, S.; Barnett, J. D. *J. Appl. Phys.* **1975**, *46*, 2774–2779.
- (11) Hutchinson, E. J.; Ben-Amotz, D. *J. Phys. Chem. B.* **1998**, *102*, 3354–3362.
- (12) Ben-Amotz, D.; Herschbach, D. R. *J. Phys. Chem.* **1990**, *94*, 1038–1047.
- (13) Ben-Amotz, D.; Willis, K. W. *J. Phys. Chem.* **1993**, *97*, 7736–7742.
- (14) Atkins, P. W. *Physical Chemistry*, 6th ed.; Oxford University Press: New York, 1998.
- (15) Jannasch, H. W.; Mottl, M. J. *Science* **1985**, *229*, 717–725.
- (16) Chyba, C. F. *Nature* **2000**, *403*, 381–382.
- (17) Florian, J.; Warshel, A. *J. Phys. Chem. B* **1999**, *103*, 10282–10288.
- (18) Rashin, A. A.; Bukatin, M. A.; *Biophys. Chem.* **1994**, *51*, 167–192.
- (19) Ben-Naim, A. *Biopolymers* **1975**, *14*, 1337. Ben-Naim, A. *J. Phys. Chem.* **1978**, *82*, 874–885.
- (20) Grunwald, E.; Steel, C. *J. Am. Chem. Soc.* **1995**, *117*, 5687–5692.
- (21) Lee, B. *Biophys. Chem.* **1994**, *51*, 271–278.
- (22) Tapia, O.; Bertran, J. *Solvent Effects and Chemical Reactivity*; Kluwer Academic Publishers: Boston, 1996.
- (23) Hanson, J. P.; McDonald, I. R. *Theory of Simple Liquids*; Academic Press: New York, 1986.
- (24) Chandler, D. *Introduction to Modern Statistical Thermodynamics*; Oxford University Press: New York, 1987; 209–213.